Combining XRF and GRT for the analysis of ancient silver coins☆

F.J. Ager [a,b,*], B. Gómez-Tubío [a,c], A. Paúl [d], A. Gómez-Morón [e], S. Scrivano [a], I. Ortega-Feliu [a], M.A. Respaldiza [a,f]

[a] *Centro Nacional de Aceleradores (CNA), Universidad de Sevilla-CSIC-Junta de Andalucía, Seville, Spain*
[b] *Departamento de Física Aplicada I, University of Seville, Seville, Spain*
[c] *Departamento de Física Aplicada III, University of Seville, Seville, Spain*
[d] *Department of Mechanic and Material Engineering, University of Seville, Seville, Spain*
[e] *Instituto Andaluz de Patrimonio Histórico, Seville, Spain*
[f] *Departamento de Física Atómica, Molecular y Nuclear, University of Seville, Seville, Spain*

abstract

Archaeological silver–copper alloys are usually affected by silver enrichment of the near surface layers, either intentional or fortuitous. In previous studies we have shown that surface composition of archaeological bronzes and leaded copper coins obtained by XRF can be corrected by means of gamma-ray transmission (GRT) to obtain the bulk composition. In the present work, we have studied the applicability of this method to silver–copper alloys and established the most suitable conditions for the GRT correction calculation. The analysis of the microstructure of the core and the corrosion layers of a set of silver roman coins shows that copper could be leached from the surface during corrosion and cleaning treatments, resulting in an apparent silver surface enrichment. After the correction calculations by GRT method, the concentrations of the major elements, Ag and Cu, were found to be in good agreement with the bulk composition obtained by direct analysis of the cut cross-sections of the coins. The GRT method shows to be a useful tool to study metal artefacts having a surface composition modified by corrosion or cleaning treatments.

1. Introduction

The application of analytical techniques in art and archaeology poses a major problem when dealing with invaluable objects because sampling, cutting, polishing or any kind of modification is unacceptable. Consequently, a non-destructive analysis is the only possible approach. The traditional non-destructive surface analytical techniques for this field are based on the measurement of characteristic X-rays: X-ray fluorescence analysis (XRF), electron probe microanalysis (EPMA), X-ray microanalysis in a scanning electron microscope (SEM–EDX), synchrotron micro-X-ray fluorescence analysis (SRXRF) and particle-induced X-ray emission (PIXE). In addition, neutron activation analysis (NAA) and, more recently, deep proton activation analysis (DPAA) are occasionally used as well. However, surface techniques have to be used with caution especially in the case of the determination of the composition of ancient alloys, because only a surface layer of limited depth, typically from 1–2 μm to 20–30 μm, is analyzed. The surface of ancient alloys may have been altered by diverse factors, including the manufacturing process, corrosion, oxidation and cleaning treatments, and its composition may not be representative of the bulk material. In most cases, the bulk composition cannot be measured directly.

For example, ancient silver–copper alloys are known to be frequently affected by apparent silver surface enrichment [1–14], and the extension in depth of this enrichment can reach several hundreds of microns, far beyond the penetration depth of surface techniques. The precise knowledge of the composition of ancient silver–copper coins is necessary in order to assess the genuine fineness of the alloy, and also the relative proportion of major elements provides valuable information on changes in monetary policies, economic changes and materials technology.

In ancient Ag–Cu coins, corrosion primarily affectsthe copper-rich phase. The main corrosion product formed on ancient silver–copper coins is copper oxide (Cu_2O). Thus, silver enrichment at the surface is usually the consequence of the preferential corrosion of copper due to its higher electronegativity relative to silver. During this corrosion process, copper could be leached [4,7,15], resulting in the preferential Cu depletion and the apparent enrichment of Ag at the surface. Different studies of the corrosion performed on cross-sections of ancient coins, by SEM/EDX, XRF and/or PIXE [5,7,8,12,16–19], revealed differences up to 50% between the composition of the core and the surface. Specifically, for corroded ancient coins with bulk concentrations of 20%–71% Ag, surface concentrations of 80%–95% have been found [4,7,18]. For higher bulk concentrations (72%–92% Ag), even higher surface concentrations have been found (up to 99% Ag). Some authors have also

BORRADOR

indicated that Ag enrichment can be deliberately carried out during manufacturing processes [7], and usual chemical cleaning treatments contribute similarly to this surface enrichment [17], although it is difficult to determine the weight of each contribution together with corrosion in ancient coins. Therefore, non-destructive surface analysis methods alone should not be directly used to determine the fineness of ancient Ag–Cu coins, unless the reliability of the results can be ensured using a complementary methodology.

Several non-destructive approaches have been proposed to provide reliable bulk compositional data. By calculating the ratio of the Ag–K/Ag–L intensities obtained by one of the fluorescence techniques it is possible to estimate the degree of surface silver enrichment and the error occurring because of it [4,5,9,13,18,20]. Other methodologies are usually based on a combination of several techniques: XRF/EPMA–EDS [4], RBS/PIXE [17], XRF/PIXE/SEM–EDX [18], PIXE/NAA [21], XRF/PIXE/NAA [22,23], and XRF/PIXE/DPAA [24]. However, most of those methods are only aimed at estimating the error or detecting a possible silver surface enrichment and then select the unaffected reliable measurements.

A new approach is proposed in this study: the determination of the composition of the bulk material by means of the correction of surface concentrations using non-destructive volume techniques. In previous works by our group [25–28], the combination of PIXE or XRF with gamma-ray transmission (GRT) was successfully applied to the analysis of archaeological bronzes. Ancient bronze artefacts and coins were analyzed in order to perform a correction to the surface composition, highly altered by corrosion, with the knowledge of the gamma-ray attenuation coefficient of the sample, and so obtain the composition of the bulk material.

The purpose of this work is to study the applicability of this method to silver–copper alloys. A microstructural analysis by optical metallography and SEM–EDX was also performed to observe the phase composition of the corroded layers and the bulk alloy and hence to determine the appropriate variables for GRT correction calculations. The surface concentrations of a set of silver roman coins obtained by XRF [12] were corrected by means of GRT measurements and the results were compared with the concentrations obtained by direct micro-XRF analysis of cross-sections of the coins.

2. Materials and methods

2.1. Coins analyzed and sample preparation

Five Roman Republican coins, 3 denarii (N2, N8 and N9) and 2 victoriati (N10 and N11), from 211 BC to 86 BC [12] were analyzed. Surface elemental composition of these coins was determined by means of XRF and corrected by GRT. In order to determine the bulk composition directly, coins were cross-sectioned by an automated diamond saw, polished with diamond solutions up to 1 μm and then analyzed by micro-XRF.

The microstructure was studied by a combination of SEM–EDX and optical microscopy (OM). The cut cross-sections of the coins were embedded in epoxy resin, grinded to 1000 grit SiC paper and mirror polished using 0.1 μm and 0.03 μm alumina powder. After SEM–EDX analysis, samples were etched with aqua regia ($HNO_3 + 3HCl$) to reveal the different grains and phases within the structure under OM inspection.

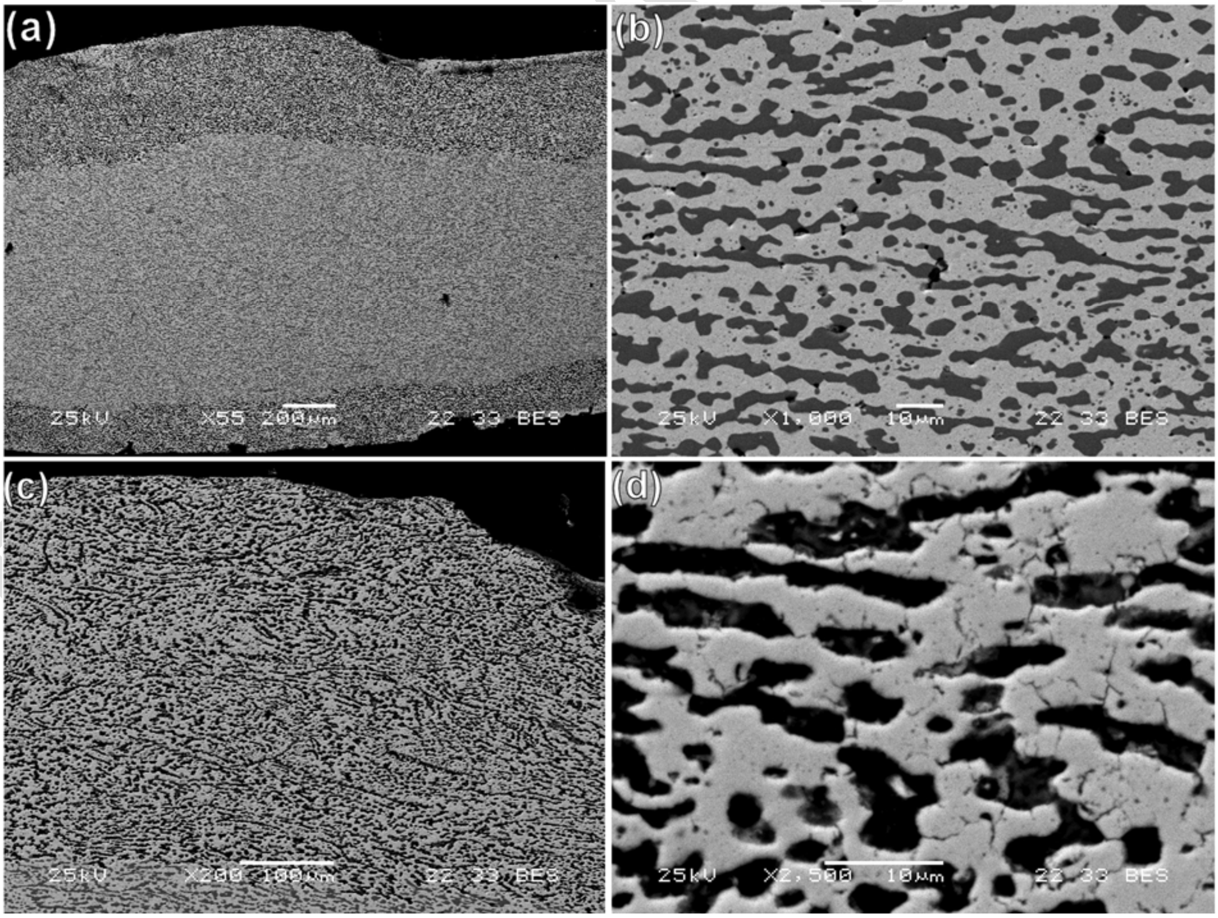

Fig. 1. SEM images of the cut cross-section of victoriatus N11. (a) General view showing the homogeneous core surrounded by a variable corrosion layer. (b) Enlargement of the core region: bright areas correspond to the silver-rich phase and dark areas, to the copper-rich phase. (c, d) Enlarged views of the corrosion layer: the dark copper-rich phase is almost completely lost.

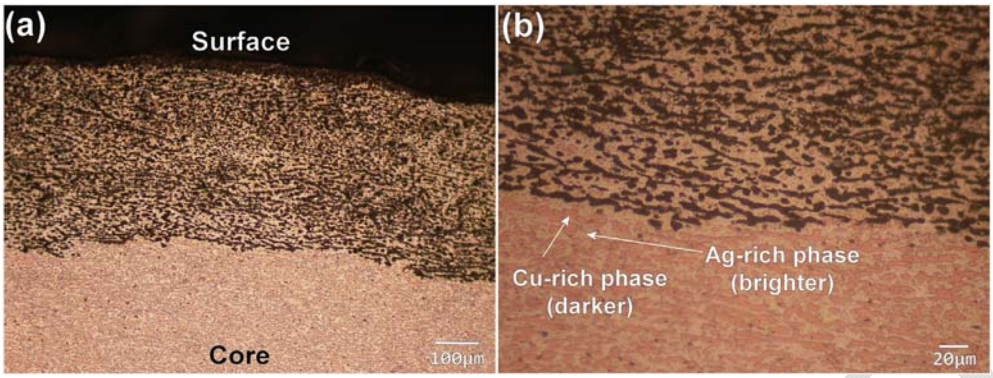

Fig. 2. OM images of the metallographic structure of coin N11. (a) General view showing the corrosion layer and the core of the coin. (b) Detail of the interface: the brighter areas of the core correspond to the Ag-rich α-phase and the darker areas, to the Cu-rich β-phase (almost lost in the corrosion layer).

2.2. Instrumentation

The XRF spectrometer is based on a portable X-ray tube (EIS XRG35) with a W anode, 1 mm diameter beam and 1 mm thick Al filter. The analyses were performed at 30 kV and 590 μA in normal incidence. The micro-XRF experimental setup consists of a low power (30 W) air-cooled micro-focus portable X-ray source (iMOXS-MFR) [29] with a Rh anode (50 kV, 800 μA), combined with a polycapillary mini-lens in the excitation channel (50 μm beam diameter at 7.5 keV). In the detection channels, silicon drift detectors (SDD) were used. More detailed experimental conditions of XRF and micro-XRF can be found elsewhere [12].

The experimental GRT setup [25–28] consisted of a ^{241}Am point gamma-source (60 keV, 3.7 GBq) of 6 mm diameter, properly shielded with lead and collimated to a 4 mm diameter beam. The transmitted gamma-rays from the source were detected with a NaI(Tl) detector surrounded by copper plates to absorb Pb X-rays from the shielding. Coin densities were measured with a He pycnometer (Accupyc II 1340).

SEM–EDX analysis of the cross-sections was performed by using a scanning electron microscope JEOL, model JSM-6460 LV with INCA X-sight software (EDX–SEM). Images were obtained with backscattered electrons (BSE) at 25 kV.

2.3. GRT correction calculation

The GRT correction method [25,26] is based on the hypothesis that one of the elements (called "main element") is affected by surface corrosion in a different way than the rest of them, so the sample can be treated as a binary compound of that particular element and an artificial "element" composed of the mixture of the rest of them, called "mixture element". With this assumption, the mass attenuation coefficient of the mixture μ_{mixture} is theoretically calculated by using Bragg's additivity law applied to the surface concentrations given by XRF. This coefficient, together with the mass attenuation coefficient μ measured directly by GRT, allows correcting the XRF concentrations of the elements in the bulk.

The right choice of the main element is essential for this calculation, but it will depend on the corrosion mechanisms of the alloy. In silver–copper alloys, copper should be considered as the main element due to its preferential corrosion and subsequent loss to the environment by leaching mechanisms, as mentioned before, even though silver is often the major alloy constituent. Thus, the "mixture element" is composed of surface elements not affected by corrosion and their relative proportions can be assumed to be approximately the same as in the bulk material. In the case of ancient coins, microstructural and metallographic analyses can provide important information about the corrosion process to confirm this choice.

For this study, the mass attenuation coefficient in the central coin region was obtained by GRT. However, the calculation of μ is dependent on the sample density, and the possible porosity of the corroded surface may affect the density measurements. To prevent the effect of the porosity, coin densities were determined with a He pycnometer. The average thickness was also calculated in the central region. A total of 4 to 6 points were analyzed on the same surface region by XRF, on both obverse and reverse. The composition of each point was corrected and then averaged to obtain the mean corrected composition.

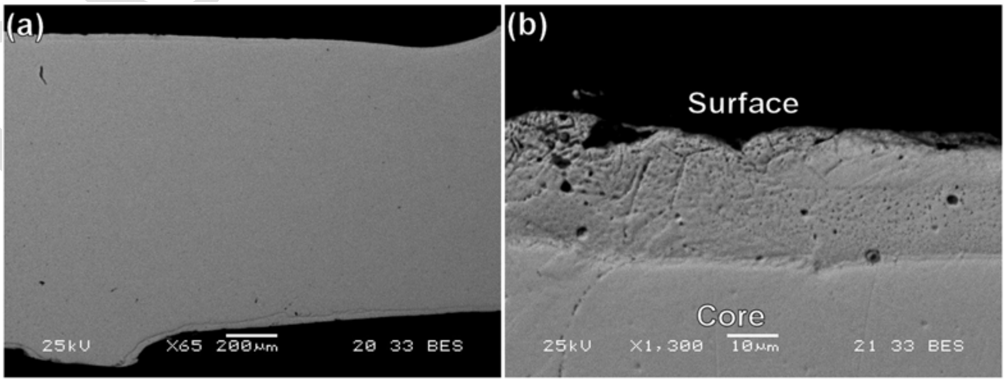

Fig. 3. SEM images of the cut cross-section of denarius N2. (a) General view showing a homogeneous single phase core with a very thin corroded layer. (b) Enlarged view of the outermost layers: the corrosion layer is affected by inter- and intragranular corrosion.

BORRADOR

3. Results and discussion

3.1. *Microstructural and metallographic analyses*

The microstructure of the victoriati is very different from that of the denarii. SEM micrographs of victoriatus N11 (Fig. 1) and the corresponding metallographic inspection (Fig. 2) show a homogeneous core surrounded by an outer corroded layer with a thickness of about 500 μm on one side and 200 μm on the other. The difference is probably due to burial conditions, so one side would have been more exposed to moisture than the other.

Coin N11 presents a very fine-sized grain structure of about 5 μm, formed by two phases (Fig. 1a and b): a bright silver-rich α-phase (Ag N 90%) and a dark copper-rich β-phase (Cu N 90%). The phase proportion (77% α–23% β) is very similar to the eutectic composition (72% α–28% β), and therefore the microstructure seems to correspond to a eutectic structure, with the grains elongated along the line of deformation of the coin, probably due to striking of the blanks during the minting process. The darker phase is almost completely lost in the outer corroded layer (Fig. 1d and b) due to a selective corrosion of the β phase and resulting in the dealloying of Cu, with the subsequent Ag surface enrichment. EDX analysis gave an overall composition of 62% Ag–38% Cu for the bulk alloy and 80% Ag–20% Cu for the corroded layer. The boundary between the surface layer and the core is well defined (Fig. 2), without a transition region between both. A similar structure was found in victoriatus N10.

By contrast, denarius N2 shows a very homogeneous single phase structure (Fig. 3a) with a thin porous surface oxidised layer (25–30 μm) (Fig. 3b). EDX analysis shows a small increase in silver in the surface layer (98.6% Ag, 1.4% Cu) compared to the bulk composition (98.0% Ag, 2.0% Cu). Some areas at the interface and in the surface layer are affected by intergranular corrosion, clearly visible also in the metallographic analysis (Figs. 3b and 4), but the surface also shows signs of corrosion inside the grains resulting in a certain degree of porosity. This effect can be explained by the fact that copper tends to diffuse into the surface, forming inter- and intragranular segregates (dark green areas in Fig. 4) that preferential corrosion would eventually remove.

Consequently, the concentration of silver shows that the denarii analyzed were made of high purity silver (Ag N 92%) whereas victoriati were made of debased silver. These results also confirm that for silver of high fineness, the alloy solidifies as a single homogeneous phase and significant silver surface enrichment is not expected [3,6,7]. In contrast, below 92% Ag, the alloy will separate into two distinct phases: a silver-rich phase and a copper-rich phase, the proportion of these phases being determined by the alloy composition. Besides, high fineness coins are much less affected by corrosion in general.

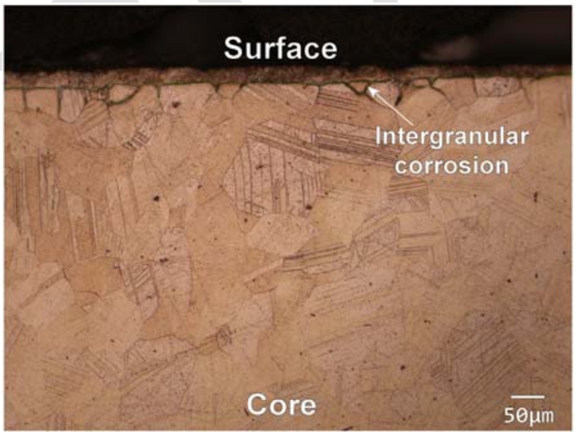

Fig. 4. OM image of the metallographic structure of coin N2. Intergranular corrosion is clearly visible at the corrosion layer–core interface.

Table 1
Theoretical (*) and measured elemental mass attenuation coefficients at 60 keV used for the calculation of GRT corrections.

	μ (cm^2/g)
Mn*	1.060(53)
Cu	1.63(26)
Ag	5.79(23)
Au	4.55(36)
Hg*	4.68(23)
Pb*	5.02(25)
Bi*	5.23(26)

3.2. *GRT correction*

The average surface composition of the coins measured by XRF and the average composition of the bulk alloy obtained directly from the cut cross-sections by micro-XRF were studied in a previous work [12]. For the correction calculation of the surface composition, Cu was chosen to be the main element due to the preferential corrosion process explained above. Only the concentration of the elements related to silver ores and metallurgy was considered in the mixture: Ag, Au, Mn, Hg, Pb and Bi. The other elements detected, such as Fe, Zn and Br, were not included in the calculation since they originate mainly from surface contamination or inclusions [30–32].

The theoretical calculation of μ_{mixture} was performed using the elemental mass attenuation coefficients at 60 keV obtained from elemental standards (Goodfellow) of some of the elements and the theoretical values from NIST [33] for the rest of them (Table 1).

Thicknesses, volumetric densities and measured values of the elemental mass attenuation coefficients μ for all coins analyzed are listed in Table 2. The densities for the calculation were obtained using a He pycnometer, although they were also measured by means of Archimedes' principle using alcohol and CCl_4 as buoyant liquids. However, the accuracy of the measurements using liquids can be compromised especially because of the porosity of certain coins. In particular, densities were underestimated by approximately 5% for coins N10 and N11, and less than 1% for coins N2, N8 and N9.

Table 3 compares the surface and bulk concentrations with the corresponding GRT corrected values. Silver and copper contents have been also represented in Fig. 5. According to these results, the correction tends to slightly underestimate the Ag contents of the high fineness denarii, N2, N8 and N9, although the bulk concentration is always within the experimental uncertainty. Copper concentration is given with a very high uncertainty because those coins are made of almost pure silver (Ag N 96%) and they cannot be considered as binary alloys being Cu as the main element. Nevertheless, high fineness silver coins can easily be discriminated by simple inspection of the corrected concentrations. If the corrected concentrations are similar to the surface composition, the latter can be considered representative of the bulk material.

GRT correction works especially well for major elements of the silver surface enriched coins N10 and N11 (victoriati). In both cases, Ag and Cu

Table 2
Thickness, density and measured total mass attenuation coefficient of the different coins.

Coin	Thickness (mm)	ρ (g/cm^3)	μ (cm^2/g)
N2	1.361(86)	10.368(62)	5.49(35)
N8	1.347(36)	9.278(56)	5.42(14)
N9	1.189(19)	10.254(62)	5.543(88)
N10	1.565(65)	9.833(59)	4.32(43)
N11	1.284(21)	9.095(55)	4.424(71)

BORRADOR

Table 3
Mean concentrations and standard deviations of the coins obtained by XRF (surface), corrected by GRT (corrected) and measured directly (bulk) in the cut cross-sections by micro-XRF.

Coin		Concentrations (wt.%)									
		Ag	Cu	Au	Mn	Fe	Zn	Br	Hg	Pb	Bi
N2	Surface	97.91(24)	1.11(17)	0.282(10)		0.085(15)	0.0170(57)		0.0108(36)	0.514(72)	0.0750(93)
	Corrected	92.4(9.8)	6.7(9.8)	0.266(30)					0.0102(36)	0.485(85)	0.071(11)
	Bulk	97.11(26)	1.66(17)	0.330(18)	0.0267(28)	0.0244(24)				0.677(97)	0.091(12)
N8	Surface	97.47(80)	0.99(32)	0.64(20)	0.23(40)	0.0483(48)	0.0368(97)	0.041(25)	0.0028(28)	0.051(13)	0.0200(77)
	Corrected	90.6(6.3)	8.1(6.3)	0.60(19)	0.22(14)				0.0026(26)	0.47(25)	0.034(18)
	Bulk	97.19(40)	1.82(35)	0.385(71)	0.09(16)	0.0244(25)			0.0282(47)	0.345(67)	0.0291(79)
N9	Surface	98.26(19)	0.563(13)	0.87(15)	0.0053(31)	0.0665(69)	0.0244(24)	0.015(10)		0.155(11)	0.0339(87)
	Corrected	93.6(5.6)	5.4(5.7)	0.83(15)	0.0051(30)					0.148(14)	0.0177(69)
	Bulk	96.24(24)	2.40(25)	0.613(81)	0.0256(30)	0.0234(47)		0.06(27)		0.470(63)	0.074(11)
N10	Surface	95.45(75)	3.79(74)	0.276(14)	0.0026(26)	0.0456(39)	0.0239(26)		0.0053(31)	0.337(29)	0.0692(60)
	Corrected	65(11)	35(11)	0.187(34)	0.0018(18)				0.0036(22)	0.229(44)	0.0469(91)
	Bulk	61.3(2.4)	38.6(2.4)		0.0485(80)			0.0009(28)			
N11	Surface	94.23(30)	4.80(29)	0.490(18)	0.0088(32)	0.109(33)	0.031(41)	0.0152(93)	0.0096(35)	0.29(20)	0.0257(26)
	Corrected	66.9(4.6)	32.5(4.6)	0.348(27)	0.0062(23)				0.0068(25)	0.205(26)	0.0183(22)
	Bulk	58.3(1.9)	41.6(1.9)		0.0572(92)						

contents tend to reproduce the concentration of the bulk. Consequently, the GRT correction method is useful in the assessment of the fineness of these silver enriched coins. Concerning trace elements, there is insufficient information because micro-XRF scans of the core of the coins were not sensitive enough to most of them. However, large differences could be expected because some trace elements, such as Pb, could have been also altered by corrosion, cleaning treatments, etc.

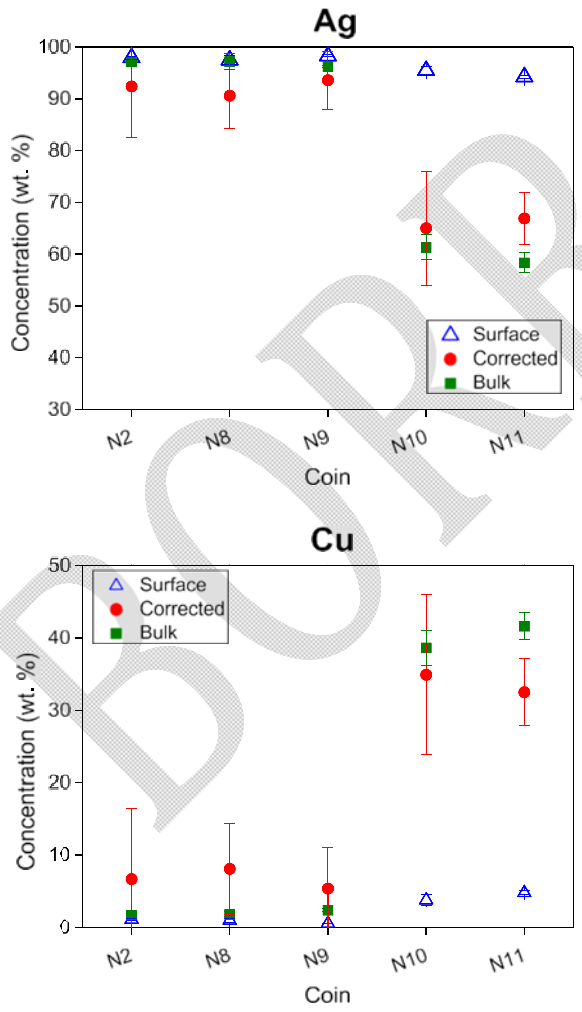

Fig. 5. Silver and copper contents (in wt.%) measured on the surface by XRF, corrected by GRT and measured directly in the cut cross-sections of the coins by micro-XRF.

4. Conclusions

The applicability of the GRT correction method to ancient silver–copper coins analyzed by non-destructive surface techniques has been established with a combination of surface, volume and microstructural analyses.

The microstructural and metallographic analyses of the cross-sections of the coins show that the surface of debased coins (victoriati N10 and N11) is affected by the preferential corrosion of copper, and they present a thick corroded outer layer where copper has been leached. As a result, an apparent silver surface enrichment is detected in these coins. On the other hand, high fineness coins (denarii N2, N8 and N9) are much less affected by corrosion and only a slight silver surface enrichment is detected.

Consequently, GRT correction calculations were based on considering copper as the main element. For high fineness coins (Ag N 96%) such as the denarii analyzed, Ag content is somewhat underestimated after correction, but the results show that surface composition is reliable enough in this case. For surface enriched coins, Ag and Cu corrected concentrations tend to reproduce the concentrations of the bulk alloy.

Finally, the GRT correction method has proven useful in the non-destructive assessment of the fineness of silver coins, either silver surface enriched or not, and hence to distinguish high fineness silver coins from debased coins. In order to improve the correction method, it would be useful to use a second gamma source with the appropriate energy, so two independent main elements (Ag and Cu) could be considered in the calculation. Unlike bronzes, where only a superficial loss of Cu can be expected because of corrosion, in silver–copper coins two major elements may be altered on the surface: Cu, again because of corrosion, and Ag, because of different enrichment mechanisms. Therefore, the assumption made by the correction method of a single main element could be insufficient in some instances. Besides, the use of a second energy allows to differentiate elements which present similar mass attenuation coefficients at 60 keV (for Ag, Pb and Bi, $\mu \approx$ [5–6] cm^2/g).

Acknowledgements

We thank Pierluigi Debernardi from the CNR IEIIT Torino (Italy) for supplying the roman coins. Work was partially supported by the project HAR2012-33002 from the Spanish Ministry of Economy and Competitiveness.

BORRADOR

References

[1] L.H. Cope, Surface-silvered ancient coins, in: D.M.M.E.T. Hall (Ed.), Methods of Chemical and Metallurgical Investigations of Ancient Coinage 1972, pp. 261–278 (London).

[2] S. La Niece, Silvering, in: S. La Niece, P.T. Craddock (Eds.), Butterworth–Heinemann Publishers, 1993, pp. 201–210.

[3] C.E. King, J.P. Northover, Der Münzhort aus dem Gutshof in Neftenbach, in: H.v. Kaenel (Ed.), Zürich Denkmalpflege Archäologische Monographien 1993, p. 110.

[4] R. Klockenkämper, H. Hubert, K. Hasler, Detection of near-surface silver enrichment on Roman imperial silver coins by X-ray spectral analysis, Archaeometry 41 (1999) 311–320.

[5] R. Linke, M. Schreiner, Energy dispersive X-ray fluorescence analysis and X-ray microanalysis of Medieval silver coins, Mikrochim Acta 133 (2000) 165–170.

[6] H. Gitler, M. Ponting, The Silver Coinage of Septimius Severus and His Family (193–211 AD): A Study of the Chemical Composition of the Roman and Eastern Issues, Glaux 16, Edizioni ennere, Milano, 2003.

[7] L. Beck, S. Bosonnet, S. Reveillon, D. Eliot, F. Pilon, Silver surface enrichment of silver–copper alloys: a limitation for the analysis of ancient silver coins by surface techniques, Nucl. Instrum. Methods Phys. Res., Sect. B 226 (2004) 153–162.

[8] M. Rodrigues, F. Cappa, M. Schreiner, P. Ferloni, M. Radtke, U. Reinholz, B. Woytek, M. Alram, Further metallurgical analyses on silver coins of Trajan (AD 98–117), J. Anal. At. Spectrom. 26 (2011) 984–991.

[9] V. Kantarelou, F.J. Ager, D. Eugenidou, F. Chaves, A. Andreou, E. Kontou, N. Katsikosta, M.A. Respaldiza, P. Serafin, D. Sokaras, C. Zarkadas, K. Polikreti, A.G. Karydas, X-ray fluorescence analytical criteria to assess the fineness of ancient silver coins: application on Ptolemaic coinage, Spectrochim. Acta, Part B 66 (2011) 681–690.

[10] F.P. Romano, S. Garraffo, L. Pappalardo, F. Rizzo, In situ investigation of the surface silvering of late roman coins by combined use of high energy broad-beam and low energy micro-beam X-ray fluorescence techniques, Spectrochim. Acta B At. Spectrosc. 73 (2012) 13–19.

[11] F. Caridi, L. Torrisi, M. Cutroneo, F. Barreca, C. Gentile, T. Serafino, D. Castrizio, XPS and XRF depth patina profiles of ancient silver coins, Appl. Surf. Sci. 272 (2013) 82–87.

[12] F.J. Ager, A.I. Moreno-Suarez, S. Scrivano, I. Ortega-Feliu, B. Gomez-Tubio, M.A. Respaldiza, Silver surface enrichment in ancient coins studied by micro-PIXE, Nuclear Instruments & Methods in Physics Research Section B-beam Interactions with Materials and Atoms 306 (2013) 241–244.

[13] J.M. del Hoyo-Meléndez, P. Świt, M. Matosz, M. Woźniak, A. Klisińska-Kopacz, Ł. Bratasz, Micro-XRF analysis of silver coins from Medieval Poland, Nucl. Instrum. Methods Phys. Res., Sect. B 349 (2015) 6–16.

[14] D.R. Walker, The metrology of the roman silver coinage, British Archaeological Reports, Supplementary Series 5, 22 and 40, 1976–1978 (Oxford).

[15] K. Butcher, M. Ponting, The Metallurgy of Roman Silver Coinage: From the Reform of Nero to the Reform of Trajan, Cambridge University Press, Cambridge, 2015.

[16] R. Linke, M. Schreiner, G. Demortier, The application of photon, electron and proton induced X-ray analysis for the identification and characterisation of medieval silver coins, Nuclear Instruments & Methods in Physics Research Section B-beam Interactions with Materials and Atoms 226 (2004) 172–178.

[17] L. Beck, E. Alloin, C. Berthier, S. Reveillon, V. Costa, Silver surface enrichment controlled by simultaneous RBS for reliable PIXE analysis of ancient coins, Nucl. Instrum. Methods Phys. Res., Sect. B 266 (2008) 2320–2324.

[18] R. Linke, M. Schreiner, G. Demortier, M. Alram, Determination of the provenance of medieval silver coins: potential and limitations of X-ray analysis using photons, electrons or protons, X-Ray Spectrom. 32 (2003) 373–380.

[19] M. Rodrigues, M. Schreiner, M. Melcher, M. Guerra, J. Salomon, M. Radtke, M. Alram, N. Schindel, Characterization of the silver coins of the Hoard of Beçin by X-ray based methods, Nucl. Instrum. Methods Phys. Res., Sect. B 269 (2011) 3041–3045.

[20] S. Pessanha, M. Costa, M.I. Oliveira, M.E.M. Jorge, M.L. Carvalho, Nondestructive analysis of Portuguese "dinheiros" using XRF: overcoming patina constraints, Appl. Phys. A 119 (2015) 1173–1178.

[21] G. Demortier, F. Bodart, T. Hackens, Analyse de monnaies de bronze grecques au moyen de la méthode PIXE et par activation aux neutrons rapides. Problèmes de méthode, Revue d'Archéométrie, 1 1981, pp. 63–72.

[22] I. Brissaud, P. Chevallier, C. Dardenne, N. Deschamps, J.P. Frontier, K. Gruel, A. Taccoen, A. Tarrats, J.X. Wang, Analysis of Gaulish coins by proton induced X-ray emission, synchrotron radiation X-ray fluorescence and neutron activation analysis, Nucl. Instrum. Methods Phys. Res., Sect. B 49 (1990) 305–308.

[23] M.F. Guerra, The study of the characterisation and provenance of coins and other metalwork using XRF, PIXE and activation analysis, in: D.C.C.A. Bradley (Ed.), Radiation in Art and Archeometry, Elsevier Science B.V, Amsterdam 2000, pp. 378–416.

[24] F. Rizzo, G.P. Cirrone, G. Cuttone, A. Esposito, S. Garraffo, G. Pappalardo, L. Pappalardo, F.P. Romano, S. Russo, Non-destructive determination of the silver content in roman coins (nummi), dated to 308–311 A.D., by the combined use of PIXE-alpha, XRF and DPAA techniques, Microchem. J. 97 (2011) 286–290.

[25] M.A. Respaldiza, F. Barranco, J. Gómez-Camacho, B.M. Gómez-Tubío, M.M. Ruiz-Delgado, Combining PIXE and XRF with gamma-ray transmission to get accurate analysis of archaeological bronzes, Nucl. Instrum. Methods Phys. Res., Sect. B 50 (1990) 226–230.

[26] M.A. Respaldiza, B.M. Gómez-Tubío, A.S. del Junco, F. Barranco, C. Sáiz-Jiménez, Non-destructive analysis of archaeological bronzes by nuclear techniques, Nucl. Instrum. Methods Phys. Res., Sect. B 89 (1994) 109–113.

[27] I. Ortega-Feliu, A.I. Moreno-Suarez, B. Gomez-Tubio, F.J. Ager, M.A. Respaldiza, S. Garcia-Dils, O. Rodriguez-Gutierrez, A comparative study of PIXE and XRF corrected by gamma-ray transmission for the non-destructive characterization of a gilded roman railing, Nucl. Instrum. Methods Phys. Res., Sect. B 268 (2010) 1920–1923.

[28] A.I. Moreno-Suarez, B. Gomez-Tubio, M.A. Respaldiza, F. Chaves, I. Ortega-Feliu, M.A. Ontalba-Salamanca, F.J. Ager, Combining non-destructive nuclear techniques to study roman leaded copper coins from Ilipa (II–I centuries BC), Nucl. Instrum. Methods Phys. Res., Sect. B 269 (2011) 3098–3101.

[29] IFG, Institute for Scientific Instruments GmbH.(Rudower Chaussee 29/31, D-12489 Berlin (www.ifg-adlershof.de)).

[30] M.A. Meyer, G. Demortier, Nonvacuum analyses of silver coins (9th to 15th century A.D.), Nucl. Instrum. Methods Phys. Res., Sect. B 49 (1990) 300–304.

[31] I. Uzonyi, R. Bugoi, A. Sasianu, A.Z. Kiss, B. Constantinescu, M. Torbagyi, Characterization of Dyrrhachium silver coins by micro-PIXE method, Nucl. Instrum. Methods Phys. Res., Sect. B 161 (2000) 748–752.

[32] N. Civici, S. Gjongecaj, F. Stamati, T. Dilo, E. Pavlidou, E.K. Polychroniadis, Z. Smit, Compositional study of IIIrd century BC silver coins from Kreshpan hoard (Albania) using EDXRF spectrometry, Nucl. Instrum. Methods Phys. Res., Sect. B 258 (2007) 414–420.

[33] J.H. Hubbell, S.M. Seltzer, Tables of X-ray mass attenuation coefficients and mass energy-absorption coefficients from 1 keV to 20 MeV for elements Z = 1 to 92 and 48, Additional Substances of Dosimetric Interest, Ionizing Radiation Division PML, National Institute of Standards and Technology (NIST). U. S. Department of Commerce, Gaithersburg, MD, 1996 (avalilable at http://www.nist.gov/pml/data/xraycoef/).

BORRADOR